Selective Comminution Applied to Mineral Processing of a Tantalum Ore: A Technical, Economic Analysis

minerals

MDPI

Article

Selective Comminution Applied to Mineral Processing of a Tantalum Ore: A Technical, Economic Analysis

Lorena Guldris Leon [1,*] and Magnus Bengtsson [2]

[1] Department of Industrial and Materials Science, Chalmers University of Technology, 412 58 Gothenburg, Sweden
[2] Department of Engineering, University of Borås, 501 90 Borås, Sweden
* Correspondence: lorena.guldris@chalmers.se; Tel.: +46-72-982-0250

Abstract: There is an increasing demand to simulate and optimize the performance and profit of comminution circuits, especially in low-grade ore processing, as is the case with critical metals minerals. Recent research has shown that the optimization result is greatly influenced by quality aspects of the products, such as cost, profit, and capacity. This paper presents a novel approach to performing a multi-objective technical and economic analysis of tantalum ore processing to increase the production of critical metals minerals. The article starts with mineral composition analysis to highlight the potential of strategies for balancing the process layout for maximized production. The introduction of a combined technical and economic analysis presents the possibility of improving the profit by rearranging the mass flow given the rock's mineral composition. Results show that selective comminution can improve process capacity by 23% and decrease production cost by 10% for the presented case.

Keywords: selective comminution; tantalum ore; process design; flowsheet recommendation and design; plant efficiency; cost analysis; mass flow model

Citation: Guldris Leon, L.; Bengtsson, M. Selective Comminution Applied to Mineral Processing of a Tantalum Ore: A Technical, Economic Analysis. *Minerals* **2022**, *12*, 1057. https://doi.org/10.3390/min12081057

Academic Editors: Pei Ni, Mincheng Xu, Tiangang Wang, Junyi Pan and Yitao Cai

Received: 22 July 2022
Accepted: 19 August 2022
Published: 21 August 2022

1. Introduction

Critical metals are present at very low abundance and are challenging to extract and utilize efficiently. The rapidly growing demand for critical mineral resources worldwide requires new understandings of the exploration advances aiding in discovering new economic targets. The outstanding properties of tantalum make it a valuable metal and, in some cases, irreplaceable and essential to sectors such as the aerospace, gas and oil, nuclear and electronic industries [1]. Due to the high economic importance, medium supply risk, and poor availability of substitution materials, the growing interest places tantalum on the critical metals risk list from the British Geological Survey [2] immediately after the rare earth elements. As a consequence of the increasing global demand for this metal, there is also a need to develop more efficient mineral processing techniques [3–5].

During critical metals processing, the rock material is generally processed from the beginning of the process until the end, by means that all particles are reduced by coarse and fine comminution equipment without arranging any separation. This requires a high amount of energy to run the process at a high cost, especially in low-grade ores as in tantalum. As a result, the mineral production industry has left behind a recent decade of unusually high product prices; additionally, this issue has led to marked reductions in productivity in existing mineral industry operations [6].

The highest cost in mining operations is related to energy costs, where 70% of it is used during crushing and milling processes [7,8]. Nonetheless, the fine comminution or grinding and processing required between 80%–90% of the energy consumption, while the crushing stage consumes 5% to 7% [9–11]. Therefore, by reducing the energy requirements during the milling process, it could be possible to reduce the total amount of energy in the process.

1.1. Selective Comminution

New studies and techniques are emerging which provide an advance or benefit in mineral production, especially for low-grade ores applications, as is the case with critical metals. It has been established by other authors that depending on the processed material and its physical and chemical properties, it could be possible to separate the material early, such as a pre-concentration of the value mineral or by valueless gangue rejection at coarse sizes at the earliest stage of the process flow [12–18]. The propensity of some ores to deport metal into specific size fractions can allow for the early rejection of low-grade materials by using selective comminution, grade by size or pre-concentrations during the coarse comminution stage [14,19–25].

Selective comminution allows a pre-classification stage at an early comminution stage, which reduces the amount to final product size and consequently reduces energy [15]. The selective comminution is based on the different properties and behaviours of the minerals that form the ore. Understanding how compressional breakage influences mineral liberation and value mineral concentration is an important first step to identifying ores with suitable characteristics for preconcentration [25]. The good combination between selective comminution and subsequent classification is a promising method for the treatment of low-grade ores and old tailing dumps [15].

An early separation means that not all materials must follow all processes and machines [6,26]. By doing a pre-classification stage during an early stage of the process, it is possible to reduce the handling and further size reduction of waste material, which means reducing the mass flow rate in some parts of the process, and therefore, it will reduce the amount of water and energy required in the whole process [27–29]. The early pre-classification stage is a result of a comminution system that embraces appropriate comminution parameters as operational parameters and material properties to achieve the best process design [14,15,17]. Once the distribution of the valuable minerals and waste is evaluated as a function of the particle size (grade-by-size distribution), as is described in the previous work of the authors Leon et al. [25], it is possible to begin analyzing different plant configuration options to increase mineral production and decrease the required energy.

1.2. Crushing Plants Parameters

The goal of crushing plants is to optimize the production of specifically sized rock fractions and, in some cases, achieve a certain level of product quality to control the yield and quality of the product and the production cost. Therefore, it is necessary to use a set of several different crushers and mills whose primary purpose is to reduce the rock size to the wanted dimensions but have a different impact on the quality [30].

The operator or the control system must consider all relevant process parameters when controlling the plant. Some parameters influence the outcome greatly, while others have a lesser effect on the product [31].

The process settings can vary to achieve specific product quality. The most common change is in the crusher's closed side setting (CSS), which enables the production of rock products in the desired size range. Crusher parameters, such as stroke or eccentric speed, are rarely changed because changing them is time-consuming. Instead, these parameters are set when the crusher is initially commissioned in the crushing plant. Material characteristics also influence the quality of the product and include parameters such as feed size and distribution, which may be controllable [25].

1.3. Techno-Economic Parameters

In mineral processing, it is not uncommon to find operations that generate fewer profits than the required cost in their production process; also, there is a significant reduction in production due to the complicated conditions of the different mining companies [32]. Furthermore, many factors influence the cost of the process, such as natural factors and the technological chain in mining and processing [33]. Therefore, techno-economic analysis plays an essential role in plant design and operations. Nowadays, evaluating and decreas-

ing the mining cost is even more critical due to the higher demand for critical metals and the environmental regulations [34]. The technical analysis includes information about the material and plant, such as the particle size distribution, plant yield optimization, plant efficiency analysis, flowsheet design and liberation of minerals. On the other hand, the economic analysis considers the investment and operation cost for equipment, installation, maintenance, and replacements [34].

There is not much work investigating the effect of economic factors and criteria on the optimality of the flowsheets in the mining sector [35–37]. To our knowledge, no paper has presented a methodology to calculate cost parameters as a function of mass flow for each piece of equipment and to calculate the production cost of the plant. This paper aims to present a way to generate cost parameters for equipment so that they can be included in a process simulation that can calculate the total production cost of a circuit.

This assessment considers the crushing plant's economic and technical aspects. However, in this paper, the analysis will focus on predicting a plant configuration's yield, product quality, and process cost. This paper analyses the existing plant from a technical, economic perspective. The survey is represented by examining two cases: case 1, an existing plant (Figure 1), and case 2, showing a proposed change in the process using selective comminution techniques to achieve an early separation and classification which will improve capacity (Figure 2). The survey has analyzed the process performance as well as the economic investment. An initial economical analysis is calibrated using the survey's measurement before predicting the direct cost in case 2.

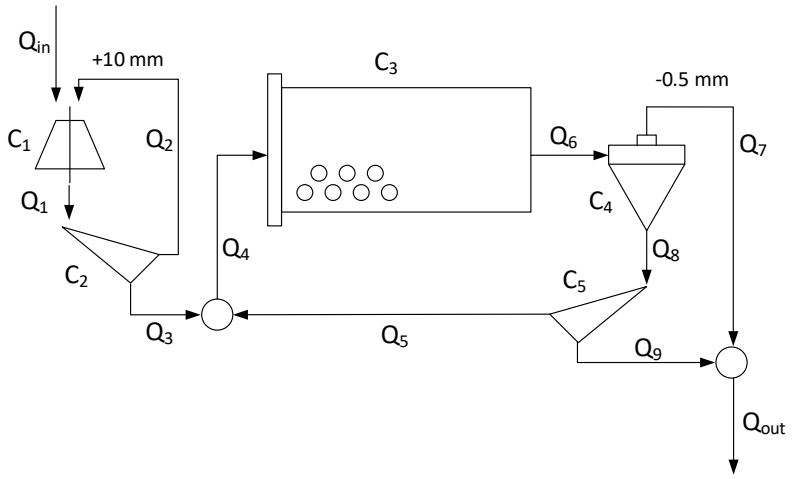

Figure 1. The configuration of the plant in Case 1.

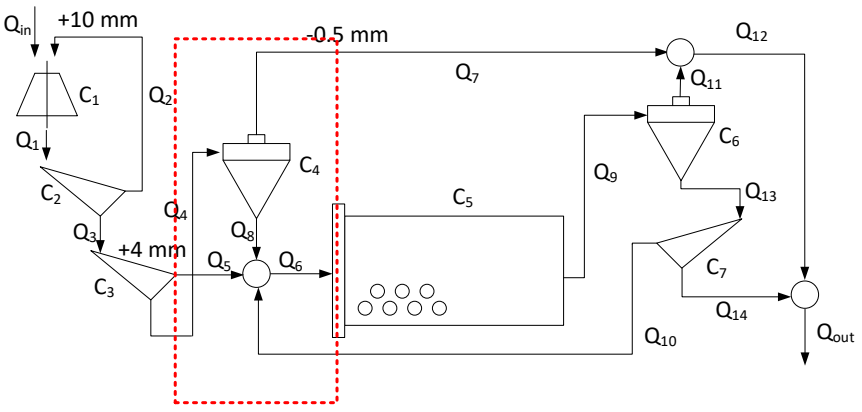

Figure 2. The configuration of the plant in Case 2.

2. Cost Analysis Bases for the Mineral Process of a Tantalum Ore

2.1. Main Application Focus

There are multiple applications for the use of the presented cost model. In this paper, the focus application will demonstrate the reduction in the energy and cost related when using a different operating scenario with varying capacities and feed size distributions, as shown in Figure 1 (traditional process flow) and Figure 2 (using selective comminution). In this paper, the principal studied application is for a tantalum low-grade ore plant, but using the same proposed methodology is possible to apply to analyze any other type of materials, being critical metals or not.

2.2. Methodology

This paper describes the methodology to evaluate the cost and production of different plant designs, considering the possibility of using selective comminution. The benefits of operating cost and production models to predict the size, mineral composition, capacity, and profit of products originates from the work by Bengtsson [38] and Leon et al. [39]. In the work of Asbjörnsson et al. [40], the importance of including the different process dynamics with the process simulation is presented. The technical and economic processes are modeled to see how the product size, capacity, and profit are affected by changes in the process parameters and process variations. The purpose is to describe the complexity of quality-driven production and to demonstrate a process model that can be used for the multi-objective optimization of a crushing plant. The process layouts used in the following simulations are shown in Figures 1 and 2.

The paper refers to previous cost functions, but more importantly, the article presents an approach so that an arbitrary cost function can be added for any equipment. Comparing the two cases assumes a linear cost model, i.e., the production cost is proportional to capacity. Furthermore, we argue that the economic model must follow the same causality as a technical model, i.e., that there must be a financial balance in the same way as, e.g., mass balance.

2.3. Theoretical Cases Analysis

The paper analyses two cases of mass flow and production cost to show how the model allows educated or well-based estimations of how a plant should be designed. Case 1 represents the traditional flowsheet of a mineral extraction process, and case 2 illustrates the use of selective comminution, where some specific size particles will be discarded during the comminution process. It is considered that all input materials and amounts are the same in each case. The only difference between these cases will be the equipment arrangement and the material division.

When analyzing the process shown in Figure 1 concerning capacity, size distribution, and energy, the feed to the ball mill contains a significant amount of 0–1 mm fraction. When isolating the size distribution of the 0–1 mm fraction in the feed distribution, the distribution bears similarities with the ball mills product. From the previous work of the authors Leon et al. [25] it is already known that in the case of the evaluated ore, the columbite-group minerals are already liberated due to the pattern of interfacial breakage, which allows the easy liberation of the minerals present in the brittle matrix.

Before the ore passes through the ball mill, it goes through a cone crusher equipped with a fine chamber, i.e., the design of that chamber. It yields a fine material that contains a high degree of liberated minerals [25]. Regarding the energy perspective, it is well known that the use of ball mills results in significant energy consumption, and therefore it would be of considerable interest to balance the overall process so that a more substantial amount of processable material can be classified prior to entering the ball mill.

2.4. Calibration Using Survey Data for Case 1

A process simulation of Case 1 was calibrated against measured data from a survey. Figure 3 compares simulated psd curves and measurements for the ball mill product (stream

Q_6) and the hydro-cyclone product (stream Q_7). The mass flow of stream Q_7 simulation value was 59 tph, and the measured mass flow 53 tph. The discharge of the hydro-cyclone represented by stream Q_8 had a simulated value of 26 tph, and the estimated mass flow was 24 tph. The hydro-cyclone used in the plant had a cut size of 0.5 mm.

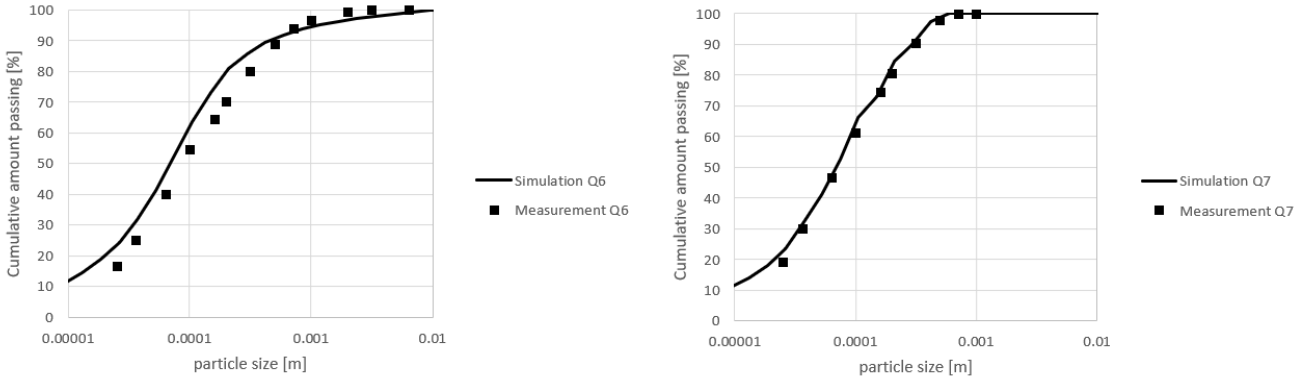

Figure 3. A comparison of psd data for the product from the mill and the hydro-cyclone.

3. Materials

The material used for the case study evaluation was a low-grade Sn-Ta greisen-type mineralization ore from the Penouta deposit located in Penouta village, in the municipality of Viana do Bola, Ourense, Galicia, in the northeast of Spain. The mineralization is hosted in leucogranite affected by greisen processes [25].

The Penouta leucogranite is hosted by metamorphic rocks, composed mainly of gneisses and mica schists [41]. The essential minerals are quartz, albite, K-feldspar, muscovite, and kaolinite. Accessory minerals are garnet, cassiterite, apatite, monazite, zircon, columbite-tantalite, and uraninite. Main valuable minerals are cassiterite (SnO_2) and columbite-group minerals (CGM), which general formula $(Fe,Mn)(Nb,Ta)_2O_6$ and four end members: columbite-(Fe), ($FeNb_2O_6$), columbite-(Mn), ($MnNb_2O_6$), tantalite-(Fe), ($FeTa_2O_6$) and tantalite-(Mn), ($MnTa_2O_6$) [42,43]. More data and characterization of this ore are presented and described by different papers as a part of multi-partner research collaboration (OPTIMORE, project number 642201) [8,25,44–52]. The sampling and characterization method which is based on these results is described in the previous work of the authors Leon et al. [25].

The case study was performed on two ~1 ton samples from the Penouta open pit mine, by collected by the OPTIMORE team of the Universitat Politècnica de Catalunya during January 2015, as a part of a multi-partner research collaboration. Due to potential mineralogical variations, samples of the mineralized leucogranite were collected from different parts of the open pit. Splits of 100 kg from the original samples were received to Chalmers University in Gothenburg during 2015. Geochemical analysis [25] indicated that valuable minerals in Penuota samples were relatively small and homogenously distributed, and it was therefore assumed that 500 g grams of starting materials would be sufficient for representative geochemical analysis. More information is presented in the previous work of the authors Leon et al. [25].

Earlier research works by Leon et al. [25,39] show that grade-by-size distribution detected a strong fractionation of metal-bearing particles into the size range of 0.125 to 1 mm, by means that the concentration of the extracted mineral will be located in that size fraction, making possible the use of selective comminution in the processing of this ore. As an example, Table 1 and Figure 4 show the mineral concentration with respect to fraction size for tantalum [39].

Table 1. Tantalum content in different size fractions of the Penouta ore after compression breakage at 30, 20 and 10% compression ratios for samples 1 and 2 [25].

Metal (ppm)	Sample No.	Compression Ratio (%)	Size Particle (mm)							
			5.6	**4**	**2**	**1**	**0.5**	**0.25**	**0.125**	**0.063**
Ta ±0.1	1	30	125	82	89	132	167	142	94	71
		20	146	109	103	163	206	135	58	52
		10	103	97	98	176	208	194	52	83
	2	30	83	72	77	136	179	132	81	80
		20	89	91	102	122	197	182	91	97
		10	111	99	112	133	201	164	84	89

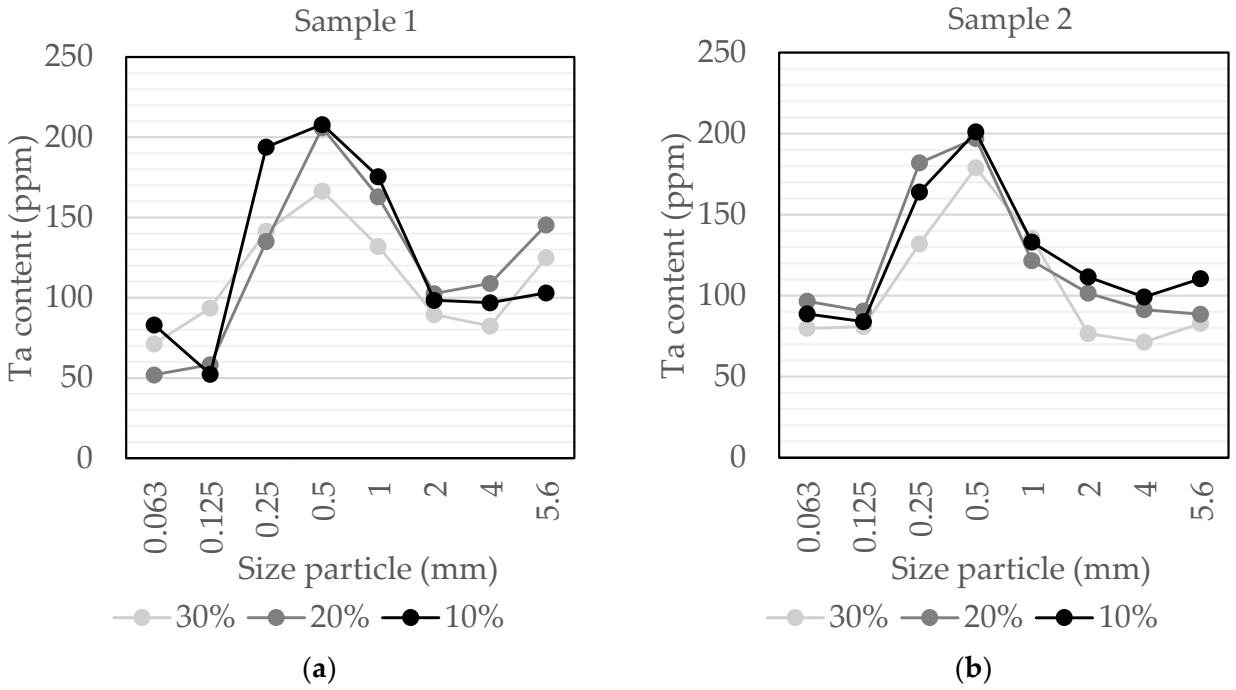

Figure 4. Representative trace elements content of the Penouta ore after compression breakage for tantalum for sample 1 (**a**) and sample 2 (**b**) from experimental data [25].

Case Study Analysis

It was established previously that depending on the processed material and its physical and chemical properties, it could be possible to use selective comminution by carrying out an early separation of the material [6,26–28]. A model for determining the cut point can be introduced if the data presented in Figure 4 is transformed into a cumulative representation shown in Figure 5. Equation (1) shows the cumulative concentration of minerals concerning the particle size x. The value b represents the slope of the exponential function. A larger b will result in a smaller top size in the screened fraction. For the experimental data presented in Figure 4, the value of b equals 1.2, i.e., the approximate top size should be $1/b = 0.833$. The value b can be determined using the linear regression model by evaluating the values for small particle sizes. This is an approximation to determine the value b. Hence, a suitable fraction of 0–1 mm will result in 67% of the minerals in this fraction. The model in Equation (1) serves as a guide for choosing a suitable fraction size for maximizing the desired mineral content; this should be combined with the requirements for the appropriate feed size for the hydro cyclone for a feasible operating condition.

$$y = \left(1 - e^{-bx}\right) \quad (1)$$

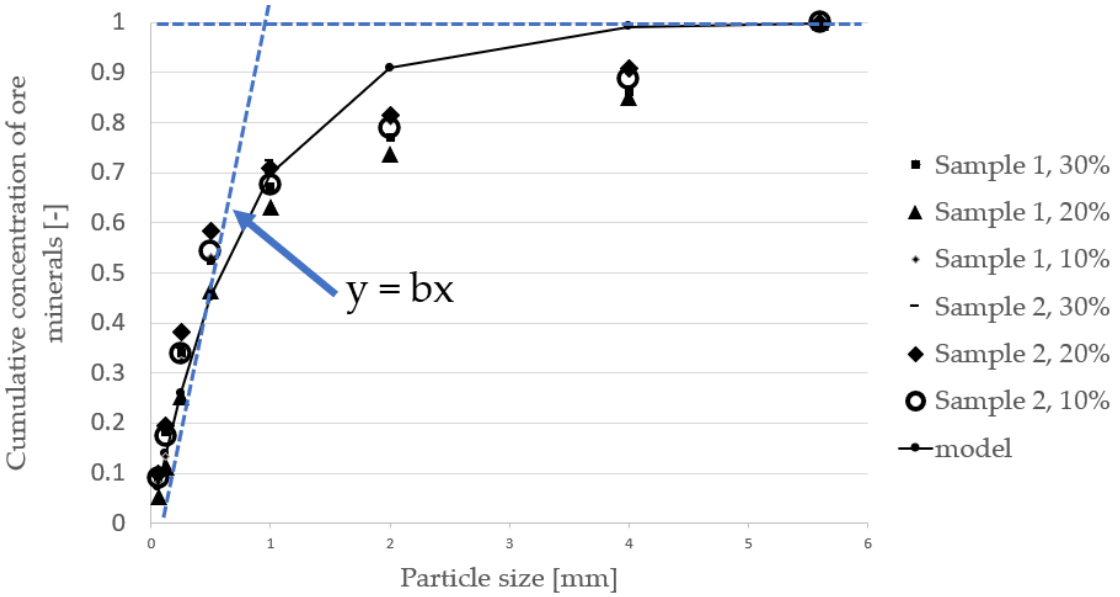

Figure 5. A cumulative analysis of tantalum content in fraction sizes from the experimental data.

If the 0–1 mm fraction could be screened and classified, as shown in Figure 5, the use of selective comminution would decrease energy usage. If selective comminution is conducted by discarding material with a low quantity of the desired mineral before entering the ball mill, a significant amount of energy can be saved. Although this process is related to the tertiary cone crushing stage, a considerable amount of liberated minerals can be harvested using a hydro cyclone.

Figure 6 shows an evaluation of the size distribution of the feed tantalum material and the resultant product in the ball mill from MATLAB simulation results using the third theory of comminution presented by Bond [53]. According to Bond, a decrease in mass flow to the ball mill by X% would directly result in an energy decrease of the same magnitude. Due to this, it suggests that there could be significant improvements by conducting a multidisciplinary process evaluation using the proposed cost model in this paper and by combining existing process simulations for PSD capacity and energy.

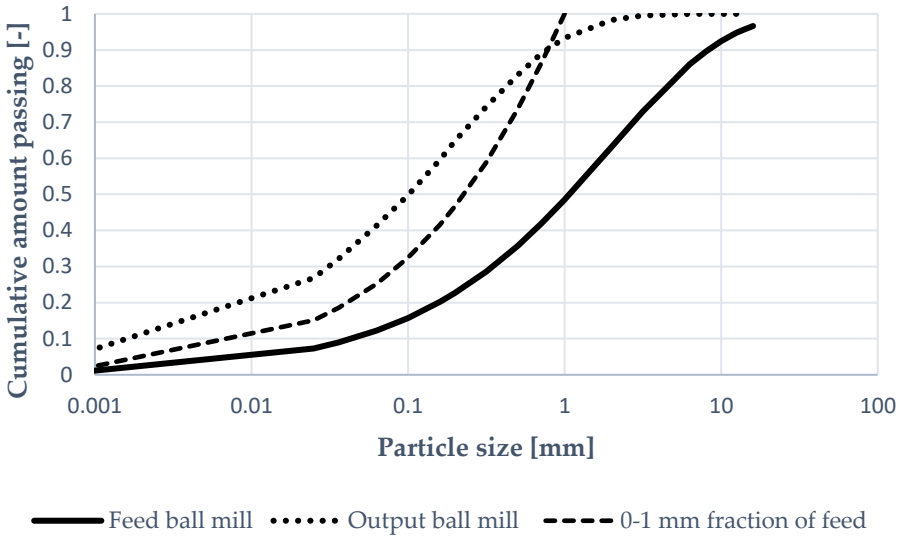

Figure 6. The size distribution of feed and product in the ball mill from MATLAB simulation results.

4. Modelling

Balancing investment costs versus circuit performance is a challenging task that relies on many different sources of information. One of these sources is process circuit simulations in which classification and screening models play an essential role. If a simple process circuit is considered, as shown in Figure 7, the cost increase per ton due to the circulating load can be derived according to work by Bengtsson et al. [54]. It is an economic benefit to keeping the recirculation of material to a minimum as it allocates costs when recirculating loads. For example, suppose the crushing stage before the ball mill is configured for optimal reduction, i.e., generates the desired number of finer particles that can be directly processed in a hydro cyclone. In that case, less material needs to be processed in the ball mill. Due to the removal of fines in the ball mill feed, it is plausible that the ball mill configuration may need to be tuned to compensate for the loss. Hence, a change in circuit design should be evaluated using process simulations to detect possible problems with size reduction due to redesign.

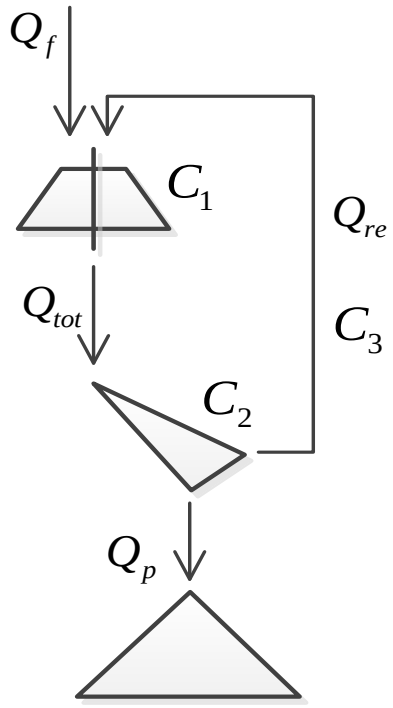

Figure 7. An introduction to the cost function.

4.1. Mass Flow Equations from a Production Perspective

A product is always associated with an undesirable action that reduces throughput. In crushing, it is often necessary to maintain certain product quality. The cost of reworking the material balances the operating cost of the crusher, screen and conveyors. On the other hand, minimizing the cost of maintenance would reduce the amount of finalized products.

Mass flow balance is performed considering the flow that goes in and out from a selected area or equipment. All material flow passing through a circuit must be the same for a steady-state, as illustrated in Equation (2).

$$Q_{in} - Q_{out} = 0 \quad (2)$$

The two cases are evaluated and stated below as an example of the mass flow equations. The operator γ represents the proportion of the feed that is split to capacity Q_i. In Equation (3), the summation γ^n represents the analytic description of calculating the power Q_1 entering the screen for a closed comminution circuit. The γ values are gathered from the particular comminution model used in the process.

Case 1:

The capacity Q_1 to Q_3 shown in Equations (3)–(5) represents the mass flow for the closed circuit of the tertiary cone crusher and the screen.

$$Q_1 = \sum_{n=0}^{m} \gamma_1^n Q_{in} \tag{3}$$

$$Q_2 = \gamma_1 Q_1 \tag{4}$$

$$Q_3 = (1 - \gamma_1) Q_1 \tag{5}$$

The capacity Q_4 represents the feed to the ball mill. Product passes a hydro cyclone and screen there will be an γ_2^n and γ_3^n multiplied within the same manner as for the closed circuit of the cone crusher and the screen.

$$Q_4 = \sum_{n=0}^{m} \gamma_2^n \gamma_3^n Q_3 \tag{6}$$

Since the process is assumed to be steady-state, the feed's mass flow will be the same as the product, as shown in Equation (7). Therefore, Equations (8) and (9) follow the same calculation pattern as presented previously, and Equations (10) and (11) represent the method for calculating the remaining mass-flow using $(1 - \gamma)$.

$$Q_6 = Q_4 \tag{7}$$

$$Q_8 = \gamma_2 Q_6 \tag{8}$$

$$Q_5 = \gamma_3 Q_8 \tag{9}$$

$$Q_7 = (1 - \gamma_2) Q_6 \tag{10}$$

$$Q_9 = (1 - \gamma_3) Q_8 \tag{11}$$

$$Q_{out} = Q_7 + Q_9 \tag{12}$$

Case 2:

The mass flow calculation of case 2 follows the same principles as case 1, but there will be an additional set of mass flows Q_4 to Q_8 see the red dotted box in Figure 2. For example, the mass flows for Q_4 to Q_8 are shown in Equations (13)–(17).

$$Q_4 = (1 - \gamma_2) Q_3 \tag{13}$$

$$Q_5 = \gamma_2 Q_3 \tag{14}$$

$$Q_6 = Q_5 + Q_8 \tag{15}$$

$$Q_7 = (1 - \gamma_3) Q_6 \tag{16}$$

$$Q_8 = \gamma_3 Q_6 \tag{17}$$

4.2. Cost Calculation

The cost calculations are based in the work by Bengtsson et al. [54]. The general cost equation has been presented in Equation (18) for the simple process circuit of Figure 7. The general equation was introduced in the work of Bengtsson et al. [54].

$$C_f = C_{tot}\left(1 + \frac{Q_{re}}{Q_f}\right) = \sum_{i=1}^{n} C_i \left(1 + \frac{Q_{re}}{Q_f}\right) \tag{18}$$

The cost calculations for Cases 1 and 2 are presented in Equations (19) and (20). The difference between the two cases is denoted by C_{bm}. C_{cc} is the cost of the cone crusher, and C_{bm} refers to the cost of the ball mill.

Case 1:

$$C_{prod} = \underbrace{C_1 + C_2 + (C_1 + C_2)\frac{Q_2}{Q_p}}_{C_{cc}} + \underbrace{C_3 + C_3\frac{Q_5}{Q_p} + C_4\frac{Q_6}{Q_p} + C_5\frac{Q_8}{Q_p}}_{C_{bm}} \quad (19)$$

Case 2:

$$C_{prod} = \underbrace{C_1 + C_2 + (C_1 + C_2)\frac{Q_2}{Q_p}}_{C_{cc}} + \underbrace{C_3 + C_4\frac{Q_4}{Q_p} + C_5\frac{(Q_5 + Q_8 + Q_{10})}{Q_p} + C_6\frac{Q_9}{Q_p} + C_7\frac{Q_{13}}{Q_p}}_{C_{bm}} \quad (20)$$

4.3. Mass Flow Equations

The modelling of the cost factors C for the comminution devices in Cases 1 and 2 is based on the survey data presented below. By isolating the investment costs and Power costs for each device, an estimate of the cost factor can be made. The cost factor for the ball mill resulted in a value of 13.1 $/tonne; for the combined circuit consisting of the hydro-cyclone and the screen, the value is 6.9 $/tonne. An assumption is made that the cost factor for the hydro- cyclone and the screen is split equally since they are placed in a serial configuration nearby each other. This results in a cost factor value of 3.45 $/tonne for the hydro-cyclone and screen separately. In Table 2, simulation results for the cost factor C_{bm} for Case 1 and Case 2 are presented. The mass flow through the ball mill in Case 1 was 85.3 tonnes/h, and for Case 2, 68.5 tonnes/h. Therefore, if the ball mill in Case 2 should have the exact utilization as in Case 1, the plant's capacity can be increased to 93.6 tonnes/hour compared to 76.3 tonnes/h in Case 1, i.e., an increase in capacity of 23%. Table 3 presents the mass flow Q for Cases 1 and 2.

Table 2. MATLAB simulation results of C_{bm} stage for Case 1 and Case 2.

US $/Tonne	Case 1	Case 2
C3	13.1	3.45
C4	3.45	3.45
C5	3.45	13.1
C6	-	3.45
C7	-	3.45
C_{bm} (calculated)	20.33	18.19
C_{bm} (survey)	20.03	17.87

Table 3. MATLAB simulation results of mass flow Q for Case 1 and Case 2.

Tonnes/h	Case 1	Case 2
Qp	76.3	76.3
Q4	87.1	27.2
Q5	10.8	49.1
Q8	31.9	11.9
Q9	-	68.5
Q10	-	7.26
Q13	-	25.1

4.4. Direct Cost Comparison

In Swart et al. [55] research, direct cost comparison for a ball mill circuit is presented. These data have been used to calibrate the cost model for each piece of equipment. However, the development in recent years of COVID and the conflict in Ukraine has affected the modelling accuracy due to the increase of the need of the metals and at the same time the increase in the cost, which affect the sector in the short and long term. Gałaś et al. [56] pointed out that the cost of production has increased due to the unpredicted costs of COVID-19, including the higher

costs of concentrate processing. Furthermore, the production's economic effect has been impacted both by COVID-19 and the lower metal prices [56].

In Table 4, the Equipment cost for Case 1 is presented. The dominant investment cost is in the ball mill, representing 80% of the investment cost. Conveyors, Screens and Hydro-cyclones are about 8% of the investment cost.

Table 4. The equipment cost for Case 1.

Equipment Cost (US$) Wet Ball Mill Circuit Case 1	
Feed conveyors	186,381
Feed weightometer	18,954
Mill (including motor)	2,482,974
Mill relining machine	325,377
Mill discharge	37,908
Hydrocyclone cluster	63,180
Total equipment cost (US$)	**3,114,774**

In Table 5, the equipment cost for case 2 is presented. The increase in infrastructure will increase the proportional cost for conveyors, screens and hydro-cyclones to 11% of the total cost and in absolute values with approximately $100,000.

Table 5. The equipment cost for Case 2.

Equipment Cost (US$) Wet Ball Mill Circuit Case 2	
Feed conveyors	223,657
Feed weightometer	18,954
Mill (including motor)	2,482,974
Mill relining machine	325,377
Mill discharge	37,908
Hydrocyclone cluster	126,360
Total equipment cost (US$)	**3,215,230**

In Table 6, the direct costs for Cases 1 and 2 are presented. The production cost for the complete ball mill circuit was 20 $/tonne for Case 1 and 17.9 $/tonne for Case 2.

Table 6. A direct cost comparison between Case 1 and Case 2.

Component Cost (US$) Wet Ball Mill Circuit	Case 1	Case 2
Purchased equipment	3,146,700	3,248,186
Purchased equipment installation	1,295,700	1,337,488
Control and Instrumentation (installed)	370,200	382,140
Piping (installed)	925,500	955,349
Electrical (installed)	370,200	382,140
Buildings (including services)	925,500	955,349
Site improvements	277,650	286,605
Service facilities (installed)	1,758,450	1,815,163
Land	185,100	191,070
Total Direct Cost (US$)	**9,255,000**	**9,553,488**
Indirect Cost (US$)	**2,000,000**	**2,064,503**
Power (7 c/kWh)	1,627,000	1,271,678
Mill drive (kW)	1200	938
Power Mill kWh	2,040,000	1,594,483
Mill (kWh/tonnes)	16	16
Mill (US$/tonnes)	11.2	11.2
Power Mill (US$)	1,428,000	1,116,138
Production cost ($/tonnes)	**20.0**	**17.9**

4.5. Sensitivity Analysis

The energy costs will drive production costs linearly since the ball mill uses the dominating energy. However, the investment cost for the new screen and hydro cyclone will be sensitive to the fluctuations in manufacturing costs. In recent years the prices have increased rapidly, and if the worst-case scenario was an increase in investment cost by 50% in new equipment, the expected production cost for case 2 would be 18.3 $/tonnes compared to 17.9 $/tonnes. Still, additional equipment investment would lower production costs by 8% compared to Case 1.

5. Results

When analyzing the processes in Cases 1 and 2, the equipment supporting the ball mill is assumed to have a significantly lower production cost than the ball mill. This is supported by the survey data presented in Section 4.4 of the direct cost comparison. Furthermore, the dominating production cost is located in the energy consumption of the ball mill. Therefore, case 1 is used as a reference case, and Case 2 represents a modification of Case 1 to enable pre-classification of 0–1 mm fraction from the cone crushing stage.

In case 2, bypassing 0–1 mm will result in a 10% decrease in production cost with the same mass flow as in Case 1.

6. Discussion

Selective comminution can be utilized when the economic perspective of new investments can be adequately evaluated. Selective comminution has demonstrated a valuable tool for reducing the energy requirements and cost during the mineral extraction of tantalum ore.

Penouta material has established an enrichment of the tantalum content in the size fractions corresponding to 0–1 mm by Leon and Bengtsson [25,39]. Using a theoretical framework allows one to analyze and understand the different plats configurations in terms of equipment, capacity, and material flow and compare them in their production cost.

Once the distribution of the valuable minerals and waste is evaluated as a function of the particle size, it is possible to begin analyzing different plant configuration options to increase mineral production and decrease the required energy. Nonetheless, there is no available tool that allows measuring the reduction in the power necessary or the cost-saving of the new process design. The proposed framework combines cost calculation analysis with existing process simulations. The combined technical and economic model helps optimize production and could be used as a tool to evaluate future investments.

By using selective comminution and bypassing 0–1 mm using a hydro-cyclone before the ball mill, the production cost decreased by 10%. The idealization used for calculating production capacity may result in a more positive change than in real-life situations. However, steady-state mass balance models for predicting the process's ability are considered reliable. Therefore, the production cost estimates may differ between the cases, and it is recommended to investigate the driving mechanisms further before using the presented technical cost analysis.

Regarding the technical cost analysis, it has been demonstrated that by insolating each direct cost, of screen, hydrocyclone and ball mill, and then calculating cost parameters of each equipment, where the parameters is a function of the mass flow. In addition, the paper presents a way to isolate each direct equipment cost by calculating a cost parameter that is used as a scaling constant in a linear function that has mass flow as a variable.

7. Conclusions

It has been shown that the implementation or evaluation of the presented technical-economic analysis considering the mass flow model in conjunction with the cost model provides a better estimation of the process performance and allows a better assessment of the equipment used in capacity and cost. Therefore, the developed theoretical framework

mining tool can analyze, optimize and evaluate the structural design regarding operating expenses and mass flow.

Two cases were presented with similar amounts of equipment but differently arranged in the process flow in the proposed study case. It was established that the different arrangements in the plant would influence the production cost. It was shown that using selective comminution and bypassing 0–1 mm using a hydro-cyclone before the ball mill can decrease the production cost by 10% and increase the mineral extraction capacity by 23% if the ball mill utilization should be the same for Case 1 and Case 2.

Selective comminution has been demonstrated to be a valuable tool for reducing the energy requirements and cost during the mineral extraction of tantalum ore.

Author Contributions: Conceptualization, M.B.; methodology, L.G.L. and M.B.; validation, M.B.; formal analysis, L.G.L. and M.B.; investigation, L.G.L. and M.B., data curation, L.G.L. and M.B., writing—original draft preparation, L.G.L. and M.B., writing—review and editing, L.G.L. and M.B., visualization, L.G.L. and M.B.; supervision, M.B.; project administration, M.B.; funding acquisition, M.B. All authors have read and agreed to the published version of the manuscript.

Funding: This work is part of the OptimOre project funded by the European Union Horizon 2020 Research and Innovation Programme under grant agreement No 642201.

Conflicts of Interest: The authors declare no conflict of interest.

References

1. Jabłońska-Czapla, M.; Grygoyć, K. Speciation and Fractionation of Less-Studied Technology-Critical Elements (Nb, Ta, Ga, In, Ge, Tl, Te): A Review. *Pol. J. Environ. Stud.* **2021**, *30*, 532. [CrossRef]
2. BGS. British Geological Survey, 2015 BGS, British Geological Survey British Geological Survey Risk List 2015, National Environmental Research Council, England. 2015. Available online: https://www.bgs.ac.uk/mineralsuk/statistics/riskList.html (accessed on 1 July 2022).
3. Hayes, S.M.; McCullough, E.A. Critical minerals: A review of elemental trends in comprehensive criticality studies. *Resour. Policy* **2018**, *59*, 192–199. [CrossRef]
4. Schulz, K.J.; Piatak, N.M.; Papp, J.F. *Niobium and Tantalum 1411339916*; US Geological Survey: Reston, VA, USA, 2017.
5. Agrawal, M.; Singh, R.; Ranitović, M.; Kamberovic, Z.; Ekberg, C.; Singh, K.K. Global market trends of tantalum and recycling methods from Waste Tantalum Capacitors: A review. *Sustain. Mater. Technol.* **2021**, *29*, e00323. [CrossRef]
6. Johnson, N.W. Existing opportunities for increasing metallurgical and energy efficiencies in concentrators. *Miner. Eng.* **2018**, *118*, 62–77. [CrossRef]
7. Norgate, T.; Haque, N. Energy and greenhouse gas impacts of mining and mineral processing operations. *J. Clean. Prod.* **2010**, *18*, 266–274. [CrossRef]
8. Nava Rosario, J.V. Caracterización del Comportamiento Cinético en Molienda de Varias Menas de Tántalo y Wolframio. Ph.D. Thesis, Universidad de Oviedo, Oviedo, Spain, 2021.
9. Jeswiet, J.; Szekeres, A. Energy consumption in mining comminution. *Procedia CIRP* **2016**, *48*, 140–145. [CrossRef]
10. Shi, F.; Kojovic, T.; Larbi-Bram, S.; Manlapig, E. Development of a rapid particle breakage characterisation device—The JKRBT. *Miner. Eng.* **2009**, *22*, 602–612. [CrossRef]
11. Wang, C.; Nadolski, S.; Mejia, O.; Drozdiak, J.; Klein, B. Energy and cost comparisons of HPGR based circuits with the SABC circuit installed at the huckleberry mine. In Proceedings of the 45th Annual Canadian Mineral Processors Operators Conference, Ottawa, ON, Canada, 22–24 January 2013; p. 121.
12. Boundy, T.; Boyton, M.; Taylor, P. Attrition scrubbing for recovery of indium from waste liquid crystal display glass via selective comminution. *J. Clean. Prod.* **2017**, *154*, 436–444. [CrossRef]
13. Hesse, M. Selective comminution for dry pre-concentration and energy saving. In *Innovation-Based Development of the Mineral Resources Sector: Challenges and Prospects*; CRC Press: Boca Raton, FL, USA, 2018; pp. 167–174.
14. Hesse, M.; Popov, O.; Lieberwirth, H. Increasing efficiency by selective comminution. *Miner. Eng.* **2017**, *103*, 112–126. [CrossRef]
15. Hesse, M.; Popov, O.; Lieberwirth, H. Selective comminution–an example of quantitative microstructural analysis as support in ore beneficiation. In Proceedings of the Selective Comminution and QMA. SAG Conference, Vancouver, BC, Canada, 20–24 September 2015.
16. Lieberwirth, H.; Popov, O.; Aleksandrova, T.; Nikolaeva, N. Scientific substantiation and practical realization of selective comminution process of polymetallic mineral raw materials. In Proceedings of the E3S Web of Conferences, Yogyakarta, Indonesia, 7–8 September 2020; p. 02003.
17. Ni, C.; Zhou, S.; Gao, J.; Bu, X.; Chen, Y.; Alheshibri, M.; Xie, G.; Li, B. Selective comminution and grinding mechanisms of spent carbon anode from aluminum electrolysis using ball and rod mills. *Physicochem. Probl. Miner. Process.* **2022**, *58*, 145667. [CrossRef]

18. Waters, K.; Marion, C.; Li, R.; Grammatikopoulos, T. The Pre-Concentration of the Nechalacho Deposit: Selective Comminution. In Proceedings of the 2017-Sustainable Industrial Processing Summit, Cancun, Mexico, 22–26 October 2017; pp. 127–141.
19. Bru, K.; Parvaz, D. Improvement of the selective comminution of a low-grade schist ore containing cassiterite using a high voltage pulse technology. In Proceedings of the Proceedings of the 29th International Mineral Processing Congress (IMPC 2018), Moscow, Russian, 17–21 September 2018; pp. 17–21.
20. Bamber, A.; Klein, B.; Pakalnis, R.; Scoble, M. Integrated mining, processing and waste disposal systems for reduced energy and operating costs at Xstrata Nickel's Sudbury operations. *Min. Technol.* **2008**, *117*, 142–153. [CrossRef]
21. Burns, R.; Grimes, A. The application of pre-concentration by screening at Bougainville Copper Limited. In Proceedings of the Proceedings AusIMM Mineral Development Symposium, Madang, Papua New Guinea, 1986.
22. Carrasco, C.; Keeney, L.; Napier-Munn, T.J. Methodology to develop a coarse liberation model based on preferential grade by size responses. *Miner. Eng.* **2016**, *86*, 149–155. [CrossRef]
23. Bowman, D.; Bearman, R. Coarse waste rejection through size based separation. *Miner. Eng.* **2014**, *62*, 102–110. [CrossRef]
24. Carrasco, C.; Keeney, L.; Walters, S. Development of a novel methodology to characterise preferential grade by size deportment and its operational significance. *Miner. Eng.* **2016**, *91*, 100–107. [CrossRef]
25. Guldris Leon, L.; Hogmalm, K.J.; Bengtsson, M. Understanding Mineral Liberation during Crushing Using Grade-by-Size Analysis—A Case Study of the Penuota Sn-Ta Mineralization, Spain. *Minerals* **2020**, *10*, 164. [CrossRef]
26. Franks, G.V.; Forbes, E.; Oshitani, J.; Batterham, R.J. Economic, water and energy evaluation of early rejection of gangue from copper ores using a dry sand fluidised bed separator. *Int. J. Miner. Process.* **2015**, *137*, 43–51. [CrossRef]
27. Ballantyne, G.; Hilden, M.; Powell, M. Early rejection of gangue—How much energy will it cost to save energy? *Comminution* **2012**, *12*, 129759564.
28. De Kretser, R.; Powell, M.; Scales, P.; Lim, J. The water efficient plant of the future: Towards a holistic process chain approach. In Proceedings of the WIM 2009, Perth, Australia, 15–17 September 2009; pp. 65–70.
29. Ballantyne, G.; Powell, M.; Tiang, M. Proportion of energy attributable to comminution. In Proceedings of the 11th Australasian Institute of Mining and Metallurgy Mill Operator's Conference, Hobart, Australia, 29–31 October 2012; pp. 25–30.
30. Napier-Munn, T.J.; Wills, B.A. *Wills' Mineral Processing Technology*; Elsevier: Amsterdam, The Netherlands, 2005.
31. Remli, S.; Fellouh, N.; Batouch, T.; Metiri, F. Optimisation of rock primary crusher yield with the use of scalper. *Int. J. Adv. Eng. Man.* **2019**, *4*, 16–20.
32. Vagonova, O.; Volosheniuk, V. Mining enterprises'economic strategies as derivatives of nature management in the system of social relations. *Sci. Bull. Natl. Min. Univ.* **2012**, 127–134.
33. Voloshyna, S.; Kostakova, L. Simulation analysis of relationship between production cost and natural environment of iron ore extraction and processing. *Sci. Bull. Natl. Min. Univ.* **2017**.
34. Huang, Z.; Mohanty, M.; Sevim, H.; Mahajan, A.; Arnold, B. Techno-economic analysis of coal preparation plant design using siu-sim simulator. *Int. J. Coal Prep. Util.* **2008**, *28*, 15–32. [CrossRef]
35. Khalesi, M.R.; Zarei, M.J.; Sayadi, A.R.; Khoshnam, F.; Chegeni, M.H. Development of a techno-economic simulation tool for an improved mineral processing plant design. *Miner. Eng.* **2015**, *81*, 103–108. [CrossRef]
36. Cisternas, L.A.; Gálvez, E.D.; Zavala, M.F.; Magna, J. A MILP model for the design of mineral flotation circuits. *Int. J. Miner. Process.* **2004**, *74*, 121–131. [CrossRef]
37. Cisternas, L.A.; Lucay, F.; Gálvez, E.D. Effect of the objective function in the design of concentration plants. *Miner. Eng.* **2014**, *63*, 16–24. [CrossRef]
38. Bengtsson, M.; Asbjörnsson, G.; Hulthén, E.; Evertsson, M. Towards dynamical profit optimization of comminution circuits. *Miner. Eng.* **2017**, *103–104*, 14–24. [CrossRef]
39. Leon, L.G.; Bengtsson, M.; Evertsson, M. Analysis of the concentration in rare metal ores during compression crushing. *Miner. Eng.* **2018**, *120*, 7–18. [CrossRef]
40. Asbjörnsson, G.; Bengtsson, M.; Hulthén, E.; Evertsson, M. Modelling of discrete downtime in continuous crushing operation. *Miner. Eng.* **2016**, *98*, 22–29. [CrossRef]
41. Anticoi, H.; Guasch, E.; Hamid, S.A.; Oliva, J.; Alfonso, P.; Garcia-Valles, M.; Bascompta, M.; Sanmiquel, L.; Escobet, T.; Argelaguet, R. Breakage function for HPGR: Mineral and mechanical characterization of tantalum and tungsten ores. *Minerals* **2018**, *8*, 170. [CrossRef]
42. Černý, P.; Ercit, T. Mineralogy of niobium and tantalum: Crystal chemical relationships, paragenetic aspects and their economic implications. In *Lanthanides, Tantalum and Niobium*; Springer: Berlin/Heidelberg, Germany, 1989; pp. 27–79.
43. Martins, T.; Lima, A.; Simmons, W.B.; Falster, A.U.; Noronha, F. Geochemical fractionation of Nb–Ta oxides in Li-bearing pegmatites from the Barroso–Alvão pegmatite field, Northern Portugal. *Can. Mineral.* **2011**, *49*, 777–791. [CrossRef]
44. López, F.A.; García-Díaz, I.; Rodríguez Largo, O.; Polonio, F.G.; Llorens, T. Recovery and purification of tin from tailings from the Penouta Sn–Ta–Nb deposit. *Minerals* **2018**, *8*, 20. [CrossRef]
45. Ahmad Hamid, S.; Alfonso, P.; Oliva, J.; Anticoi, H.; Guasch, E.; Hoffmann Sampaio, C.; Garcia-Vallès, M.; Escobet, T. Modeling the liberation of comminuted scheelite using mineralogical properties. *Minerals* **2019**, *9*, 536. [CrossRef]
46. González, T.L.; Polonio, F.G.; Moro, F.J.L.; Fernández, A.F.; Contreras, J.L.S.; Benito, M.C.M. Tin-tantalum-niobium mineralization in the Penouta deposit (NW Spain): Textural features and mineral chemistry to unravel the genesis and evolution of cassiterite and columbite group minerals in a peraluminous system. *Ore Geol. Rev.* **2017**, *81*, 79–95. [CrossRef]

47. Ghorbani, Y.; Fitzpatrick, R.; Kinchington, M.; Rollinson, G.; Hegarty, P. A process mineralogy approach to gravity concentration of Tantalum bearing minerals. *Minerals* **2017**, *7*, 194. [CrossRef]
48. Hamid, S.A.; Alfonso, P.; Anticoi, H.; Guasch, E.; Oliva, J.; Dosbaba, M.; Garcia-Valles, M.; Chugunova, M. Quantitative mineralogical comparison between HPGR and ball mill products of a Sn-Ta ore. *Minerals* **2018**, *8*, 151. [CrossRef]
49. Anticoi, H.; Guasch, E.; Ahmad Hamid, S.; Oliva, J.; Alfonso, P.; Bascompta, M.; Sanmiquel, L.; Escobet, T.; Escobet, A.; Parcerisa, D. An improved high-pressure roll crusher model for tungsten and tantalum ores. *Minerals* **2018**, *8*, 483. [CrossRef]
50. Alfonso, P.; Hamid, S.; García-Vallès, M.; Llorens, T.; Moro, F.L.; Tomasa, O.; Calvo, D.; Guasch, E.; Anticoi, H.; Oliva, J. Textural and mineral-chemistry constraints on columbite-group minerals in the Penouta deposit: Evidence from magmatic and fluid-related processes. *Mineral. Mag.* **2018**, *82*, S199–S222. [CrossRef]
51. López-Moro, F.J.; Polonio, F.G.; González, T.L.; Contreras, J.L.S.; Fernández, A.F.; Benito, M.C.M. Ta and Sn concentration by muscovite fractionation and degassing in a lens-like granite body: The case study of the Penouta rare-metal albite granite (NW Spain). *Ore Geol. Rev.* **2017**, *82*, 10–30. [CrossRef]
52. Alfonso, P.; Hamid, S.A.; Anticoi, H.; Garcia-Valles, M.; Oliva, J.; Tomasa, O.; López-Moro, F.J.; Bascompta, M.; Llorens, T.; Castro, D. Liberation characteristics of ta–sn ores from penouta, nw spain. *Minerals* **2020**, *10*, 509. [CrossRef]
53. Bond, F.C. The Third Theory of Comminution. *Trans. AIME Min. Eng.* **1952**, *193*, 484–494.
54. Bengtsson, M.; Hulthén, E.; Evertsson, C. Cost And Performance Optimization of a Tertiary Crushing Stage. In Proceedings of the ESCC 2015 Conference, Gothenburg, Sweden, 7–11 September 2015.
55. Swart, C.; Gaylard, J.M.; Bwalya, M.M. A Technical and Economic Comparison of Ball Mill Limestone Comminution with a Vertical Roller Mill. *Miner. Process. Extr. Metall. Rev.* **2022**, *43*, 275–282. [CrossRef]
56. Gałaś, A.; Kot-Niewiadomska, A.; Czerw, H.; Simić, V.; Tost, M.; Wårell, L.; Gałaś, S. Impact of Covid-19 on the mining sector and raw materials security in selected European countries. *Resources* **2021**, *10*, 39. [CrossRef]